$$\langle j_n \rangle_{ds} = \sum_p \sum_{p'} [(C_{3d})_p (C_{4s})_{p'} (2n_{3d})_p!]^{-1/2} \times [(2n_{4s})_{p'}!]^{-1/2} [(2\zeta_{3d})_p]^{(n_{3d})_p + 1/2} \times [(2\zeta_{4s})_{p'}]^{(n_{4s})_{p'} + 1/2} \int_0^\infty r^{(n_{3d})_p + (n_{4s})_{p'} - 2} \times \exp\{-[(\zeta_{3d})_p + (\zeta_{4s})_{p'}]r\} j_n(sr) r^2 dr,$$

where the constants $(n_{3d})_p$, $(\zeta_{3d})_p$, $(C_{3d})_p$, $(n_{4s})_{p'}$, $(\zeta_{4s})_{p'}$ and $(C_{4s})_{p'}$ are given by Clementi (1965), and $j_n(sr)$ is the nth-order spherical Bessel function. Since the 4s orbital wavefunction of Cu^+ ions is not given in Clementi's table, that of the neutral Cu atom with the electronic configuration $(1s)^2(2s)^2(2p)^6(3s)^2(3p)^6(3d)^{10}(4s)^1$ was employed in the present study.

References

BECKER, P. J. & COPPENS, P. (1974*a*). *Acta Cryst.* A**30**, 129–147.
BECKER, P. J. & COPPENS, P. (1974*b*). *Acta Cryst.* A**30**, 148–153.
BECKER, P. J. & COPPENS, P. (1975). *Acta Cryst.* A**31**, 417–425.
BOND, W. L. (1951). *Rev. Sci. Instrum.* **22**, 344.
CLEMENTI, E. (1965). *Tables of Atomic Functions.* Supplement to *IBM J. Res. Dev.* **9**, 2–19.
FUKAMACHI, T. (1971). *Tech. Rep. Inst. Solid State Phys.* B**12**, 20.
International Tables for X-ray Crystallography (1974). Vol. IV. Birmingham: Kynoch Press.
ISHIGURO, T., ISHIZAWA, N., MIZUTANI, N. & KATO, M. (1982). *J. Solid State Chem.* **41**, 132–137.
ISHIGURO, T., KITAZAWA, A., MIZUTANI, N. & KATO, M. (1981). *J. Solid State Chem.* **40**, 170–174.
IWATA, M. (1977). *Acta Cryst.* B**33**, 59–69.
KADOTA, S., YAMADA, I., YONEYAMA, S. & HIRAKAWA, K. (1967). *J. Phys. Soc. Jpn*, **23**, 751–756.
MARTIN, M., REES, B. & MITSCHLER, A. (1982). *Acta Cryst.* B**38**, 6–15.
ORGEL, L. E. (1966). *An Introduction to Transition-Metal Chemistry: Ligand-Field Theory*, 2nd. ed. London: Methuen.
ROGERS, D. B., SHANNON, R. D., PREWITT, C. T. & GILLSON, J. L. (1971). *Inorg. Chem.* **10**, 723–727.
STEVENS, E. D. & COPPENS, P. (1979). *Acta Cryst.* A**35**, 536–539.
TANAKA, K., KONISHI, M. & MARUMO, F. (1979). *Acta Cryst.* B**35**, 1303–1308; *errata: Acta Cryst.* (1980). B**36**, 1264.
TANAKA, K. & MARUMO, F. (1982). *Acta Cryst.* B**38**, 1422–1427.
TANAKA, K. & MARUMO, F. (1983). *Acta Cryst.* A**39**, 631–641.
TOKONAMI, M. (1965). *Acta Cryst.* **19**, 486.
WILLIS, B. T. M. (1969). *Acta Cryst.* A**25**, 277–300.

Acta Cryst. (1983). B**39**, 569–575

On the Non-Stoichiometric Ytterbium Sulphide Phase 'Yb_3S_4'

BY CARLOS OTERO DIAZ AND B. G. HYDE

Research School of Chemistry, Australian National University, GPO Box 4, Canberra, ACT 2601, Australia

(*Received* 10 *March* 1983; *accepted* 11 *April* 1983)

Abstract

Examination of ytterbium sulphides in the composition range $YbS_{1.34}$ to $YbS_{1.42}$ by electron diffraction reveals that this is not, as previously reported, a homogeneous solid-solution region with the **Yb_3S_4**-type structure. In addition to reflections characteristic of this structure there are satellite reflections which indicate a long-range modulation with a variable periodicity of approximately seven to eight times. This is confirmed by electron microscopy, the most obvious modulation direction being close to ⟨830⟩ of the **Yb_3S_4** subcell.

Introduction

With the passage of time, the number of crystalline 'homogeneous solid solutions' has decreased remarkably. On closer scrutiny, many have been resolved into sequences of closely spaced or even contiguous phases, each with a highly ordered structure derived from a simple prototype by one of a few crystallographic operations (*e.g.* Andersson & Hyde, 1982, and references therein). Others exhibit short-range order, and eventually decompose into phase mixtures (*e.g.* Bakker & Plug, 1981). Some achieve partial long-range order in the form of modulated structures, the modulation being often incommensurate with the unit cell of the prototype structure (*e.g.* Makovicky & Hyde, 1981; Yamamoto & Nakazawa, 1982; McLaren, 1978).

But there is still a residuum of phases with apparently random arrays of point defects and these also demand close scrutiny, particularly by techniques that are more sensitive than the more traditional methods such as X-ray diffraction. Perhaps the most powerful of these techniques is electron microscopy/diffraction, which has proved so successful in some of the cases already referred to. Here we will report on such a study of the phase based on Yb_3S_4.

Flahaut and co-workers reported this phase as having a continuous range of homogeneous solid

0108-7681/83/050569-07$01.50

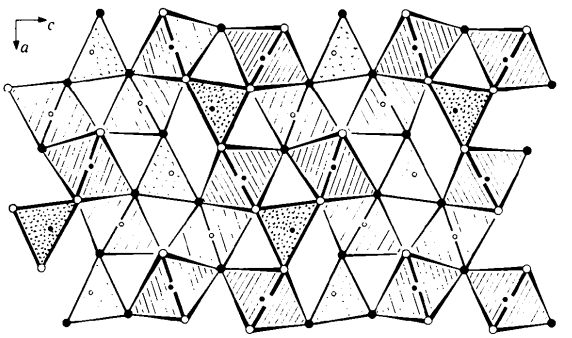

Fig. 1. The structure of Yb_3S_4 projected on (010). Large circles S, small circles Yb. All atoms at $y/b = 0$ or $\frac{1}{2}$ (open and filled circles).

solution from approximately Yb_3S_4 towards, but stopping short of, Yb_2S_3: YbS_r with $1{\cdot}33 \lesssim r \lesssim 1{\cdot}46$. This description was based on the results of X-ray diffraction studies and measurements of density and magnetic susceptibility (Domange, Flahaut, Guittard & Loriers, 1958; Flahaut, Domange, Patrie & Guittard, 1960; Flahaut, Domange, Guittard & Loriers, 1961). Single-crystal X-ray structure analysis revealed the **Yb_3S_4** structure type (Fig. 1) to be closely related to the warwickite type which may be described as **NaCl**-type ($B1$) ribbons, $4 \times 1 \times \infty$ octahedra in extent, twinned by a glide-reflection operation (Hyde, Andersson, Bakker, Plug & O'Keeffe, 1980). By this operation the 'cation deficiency' of Yb_3S_4 (25% compared to $B1$) is accommodated without recourse to cation vacancies or interstitial anions. However, the unit-cell parameters, density and magnetic-susceptibility measurements of the non-stoichiometric Yb_3S_4 phase suggest that its stoichiometric range is accommodated by a proportion of one type of cation site, the S_6 trigonal prisms, being unoccupied and in a random manner (Chevalier, Laruelle & Flahaut, 1967): $Yb^{3+}_{2+2x/3}Yb^{2+}_{1-x}\square_{x/3}S^{2-}_4$ with x varying from zero in Yb_3S_4 to 0·73 in $YbS_{1{\cdot}46}$.

Our experiments, though not yet complete, are consistent with this description except that they clearly show that the arrangement of defects is *not* random.

Experimental methods

Ytterbium sulphides were prepared by induction heating of a carbon crucible containing Yb_2O_3 in a stream of 5% H_2S + 95% argon (flow rate ~ 0·05 litre s^{-1}; pressure 10^5 Pa), followed by rapid cooling to room temperature. Temperatures were in the range 1723–2123 K and heating times varied from 40 min to 5 h. In some cases a portion of the product received further treatment: annealing for two months in a sealed evacuated silica tube at 1323 K in one case, annealing at 1773–1823 K for some hours in H_2S in another.

X-ray powder patterns of all samples (with an internal silicon standard) were obtained from a Guinier–Hägg focusing camera (Cu $K\alpha_1$, λ = 1·5405981 Å). The stoichiometry (r in YbS_r) of each sample was analysed by one or both of two methods: (*a*) electron microprobe analysis using stoichiometric Yb_2S_3 as a calibration standard, (*b*) gravimetrically; converting to stoichiometric Yb_2O_3 by heating in a thoria crucible in air at 1673 K.* Agreement between the two analytical methods was generally within the estimated experimental error for each, $\delta r = \pm 0{\cdot}01$.

Specimens (dispersed on holey carbon films on Cu grids) were studied by electron microscopy/diffraction in a JEOL 100CX instrument (tilt range ±30 or ±60°, to explore reciprocal space thoroughly) and a JEOL 200CX (for high-resolution imaging).

Experimental results

Guinier powder patterns were extremely complex (more than 100 lines in the range $6° \lesssim 2\theta \lesssim 90°$), as might be expected for the previously reported unit cell for 'Yb_3S_4': orthorhombic, space group *Pnma*, with $a \simeq 12{\cdot}7$, $b \simeq 3{\cdot}8$, $c \simeq 12{\cdot}9$ Å. A majority (but never all) of the lines could be indexed in accord with this cell, and refined unit-cell parameters were deduced. But it is clear that other phases were also present in minor amounts. Electron diffraction revealed a distinct difference between higher- (partly melted) and lower-temperature preparations, only the latter being **Yb_3Sb_4** type. The unit-cell parameters and the more reliable analyses are plotted in Fig. 2, which reveals the expected tendency

* Attempted oxygenation at lower temperatures gave compounds of formula weight higher than that for Yb_2O_3. The results at 1073 to 1273 K were consistent with the product being $(YbO)_2SO_4$, analogous to $(LaO)_2SO_4$ (Pannetier & Dereigne, 1963) but not, to our knowledge, previously reported.

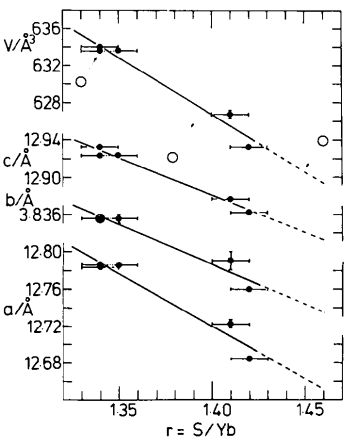

Fig. 2. Relation between stoichiometry, r in YbS_r, and parameters of **Yb_3S_4**-type subcell, a, b, c and volume V. Filled circles are present work (absence of error bars means that precision is better than size of circle); open circles are unit-cell volumes from Flahaut *et al.*

for the unit-cell axes and volume to decrease as r increases (when $3Yb^{2+} \rightarrow 2Yb^{3+} + \square_{Yb}$, Yb^{3+} being smaller than Yb^{2+}). The observed composition range, $1{\cdot}34 \lesssim r \lesssim 1{\cdot}42$ is within Flahaut's estimate of 1·33 to 1·46 (Flahaut, Domange, Guittard and Loriers, 1961).

We now consider the results of electron microscopy/diffraction. We have already noted that there are considerable differences between the electron diffraction patterns of 'low-temperature' (< ~1673 K) preparations and 'high-temperature' (> ~1673 K) preparations. One partly melted sample was subsequently annealed in H_2S at a lower temperature (1323–1373 K): it then contained both 'low-' and 'high-temperature' products. Most of the data are from low-temperature preparations. We first deal with these and then, very briefly, the rather different high-temperature specimens.

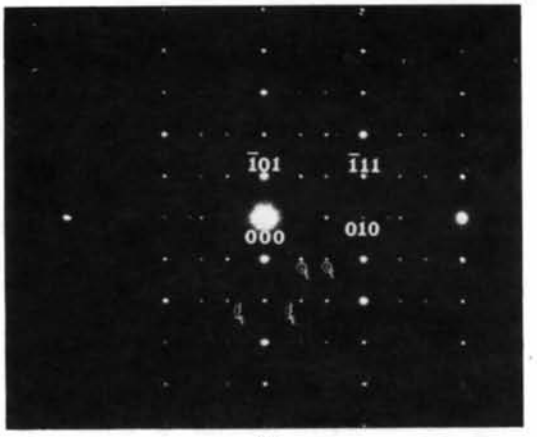

(*a*)

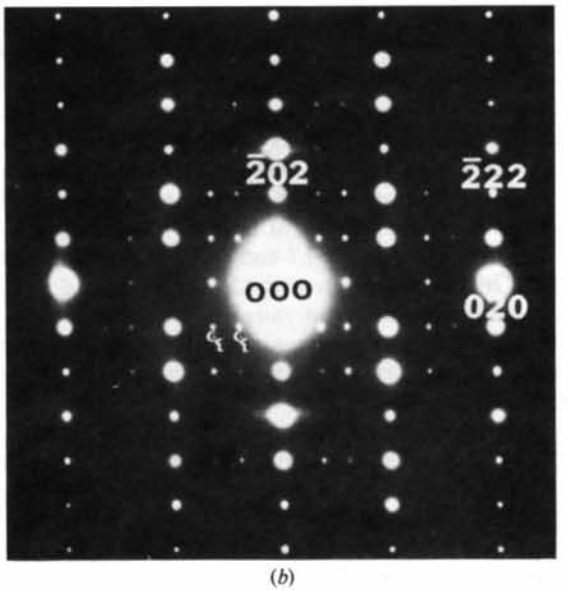

(*b*)

Fig. 3. Electron diffraction patterns from low-temperature 'Yb_3S_4' preparations; zone axes $[101]_m$ of $\mathbf{Yb_3S_4}$ subcell. Note the weak, extra *e*- and *f*-type reflections.

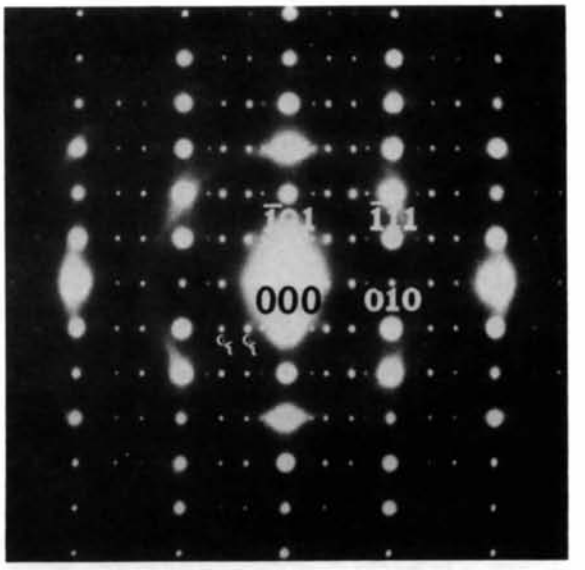

(*c*)

Fig. 3 (*cont.*) (*c*)

'Low-temperature' preparations

Electron diffraction patterns

A large proportion of diffraction patterns with appropriate zones (*cf.* below) contained two types of reflections: (*a*) 'main' reflections of high intensity, characteristic of the $\mathbf{Yb_3S_4}$ (*m*) structure type, (*b*) 'satellite' reflections of lower intensity (and not appropriate to the $\mathbf{Yb_3S_4}$ structure). The remaining patterns contain 'main' reflections only.

Several sets of diffraction patterns over a wide range of reciprocal space, each set from one crystal and with one of two reciprocal-lattice rows ($[100]_m$ or $[010]_m$) common to all, were typical of over 100 crystals examined. In each case the main reflections indexed as the $\mathbf{Yb_3S_4}$ type. These sets revealed the common characteristic, that satellites occurred in pairs along the $\mathbf{b^*}$ direction.† There are no other satellites, and hence (low-index) $[101]_m$ and $[001]_m$ zone-axis patterns were invariably used for detailed analysis, with no loss of information about the satellites.

Fig. 3 shows three typical $[101]_m$ zone-axis patterns; Fig. 4 shows three $[001]_m$ examples. (Diffuse arcs, present in some of the patterns, are due to partial decomposition of the crystal under the influence of the electron beam, and may be ignored.) These patterns (main and satellite reflections) are reminiscent of those produced from a number of other phase systems (*cf.* below) such as the plagioclase feldspars. By analogy with the analysis of diffraction patterns in those cases (McLaren, 1978) the satellite reflections in Fig. 4 may be grouped as follows:

† In some instances there may have been a *very* small deviation from exact $\mathbf{b^*}$. We will ignore this.

(i) a pair of 'e_1 satellites', first-order reflections, at the reciprocal-lattice points $(h, k + \frac{1}{2} \pm 1/\Delta, 0)$ with $h = 2n + 1$;*

(ii) a pair of 'f_1 satellites', second-order reflections, at $(h, k \pm 2/\Delta, 0)$ with $h = 2n$;

and sometimes (Fig. 4*a*):

(iii) a pair of 'e_2 satellites', third-order, at $(h, k + \frac{1}{2} \pm 3/\Delta, 0)$ with $h = 2n + 1$;

* Bown & Gay (1958) call this pair *e*.1 and *e*.2.

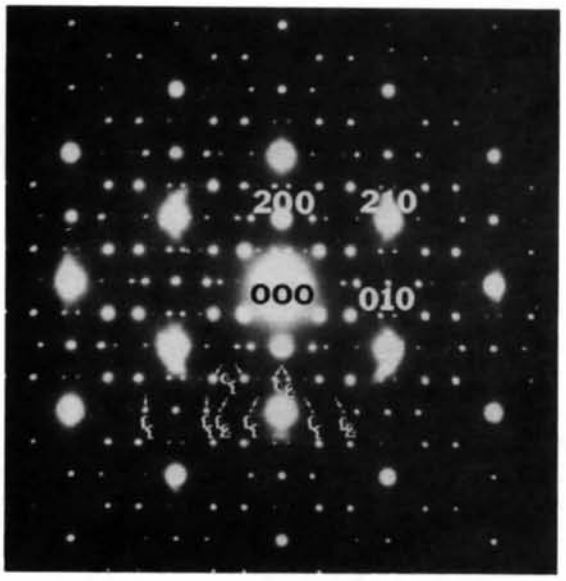

(*a*)

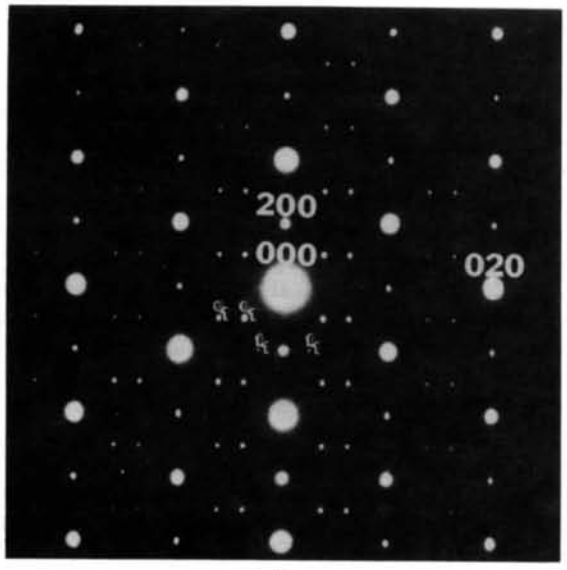

(*b*)

Fig. 4. As Fig. 3, but $|001|_m$ zones. In (*a*), (*b*) the *d* spacings corresponding to *e* and *f* reflections are incommensurate with the Yb_3S_4 subcell, in (*c*) they are commensurate.

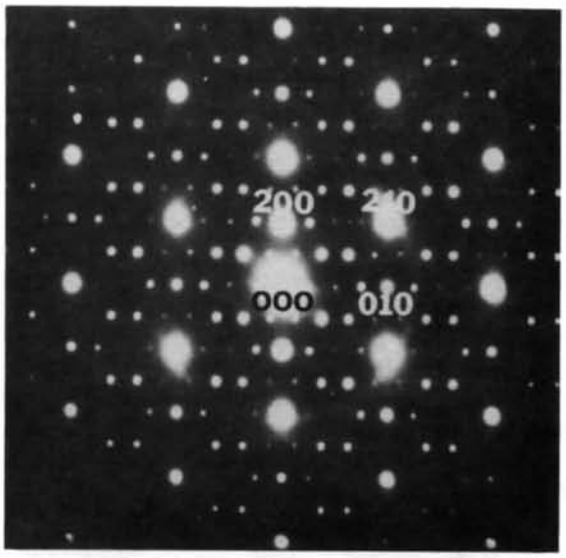

(*c*)

Fig. 4 (*cont.*) (*c*).

(iv) a pair of 'f_2 satellites', fourth-order, at $(h, k \pm 4/\Delta, 0)$ with $h = 2n$.

Values of Δ were determined by measuring the diffraction patterns.* With one exception (Fig. 4*c*) they are incommensurate with *b*.

With the benefit of hindsight it is clear that the value of Δ probably depends on both composition and temperature, and additional experiments must be made to separate the two effects. (In the present experiments the samples were prepared in H_2S and therefore the two variables are correlated because, at equilibrium, the sulphur activity depends only on the temperature.)

The available data reveal variations in Δ from crystal to crystal within a given preparation (and even within a given crystal) as well as, less surprisingly, from one preparation to another. In one sample (25 diffraction patterns from 14 different crystals) we observed a range $7{\cdot}4_0 \leq \Delta \leq 8{\cdot}5_0$, with an average value $\bar{\Delta} = 8{\cdot}00$ and a 'standard deviation' of 0·26. In another (25 diffraction patterns from eight different crystals) the range is $8{\cdot}0_6 \leq \Delta \leq 8{\cdot}4_0$ with $\bar{\Delta} = 8{\cdot}27$ and the 'standard deviation' 0·10. One crystal from a third sample had $\Delta = 8{\cdot}24$ (*i.e.* within the observed range from the first sample, from which it was prepared by annealing in a sealed tube). The one crystal from a fourth sample that was examined had $6{\cdot}9_2 \leq \Delta \leq 7{\cdot}2_5$, $\bar{\Delta} = 7{\cdot}0_1 \pm 0{\cdot}17$. Two crystals from a fifth sample had $\Delta = 7{\cdot}5_8, 8{\cdot}2_5$.

Thus Δ values are about 8, with one diffraction pattern having $\Delta = 8$ *exactly*. In that case (Fig. 4*c*) the modulation has become a (commensurate) superlattice, and the 'satellites' have transformed to relatively strong superlattice reflections.

* The accuracy in measuring Δ (from the ratio of b^* to the e_1–e_1 or f_1–f_1 satellite spacing) is $\sim \pm 0{\cdot}5\%$ or better.

Electron-microscope images

The modulation of the structure (responsible for the satellite reflections in the diffraction patterns) is not immediately obvious in the high-resolution images but it is present, as careful scrutiny reveals.

Fig. 5 is the image corresponding to the $[001]_m$ zone-axis diffraction pattern of Fig. 4(*a*), which has very well developed satellites to the fourth order, and $\Delta = 6{\cdot}9_2$. The arrowheads (in a horizontal row) indicate the approximate positions of modulations (light spots) parallel to (010), *i.e.* running vertically across the figure. They are obvious when the image is viewed along **a** at grazing incidence. The average spacing is $3{\cdot}4_5 \times \mathbf{b} = 13{\cdot}_{23}$ Å, corresponding to a modulation period of $26{\cdot}_{46}$ Å, $\Delta = 6{\cdot}9_0$ (*cf.* $6{\cdot}9_2$ from the diffraction pattern). When viewed at grazing incidence in either of the directions indicated by the pairs of arrows (approx. NW/SE and NE/SW, especially the latter) there are clearly alternating brighter and darker fringes, indicative of the same modulation. These directions correspond to the reciprocal-lattice vectors between (000) and the (two) rows of collinear satellites $e_1f_1e_2f_2$: $(\pm 7{\cdot}8_0,3,0)_m$ planes at $\pm 49°$ to $(010)_m$.

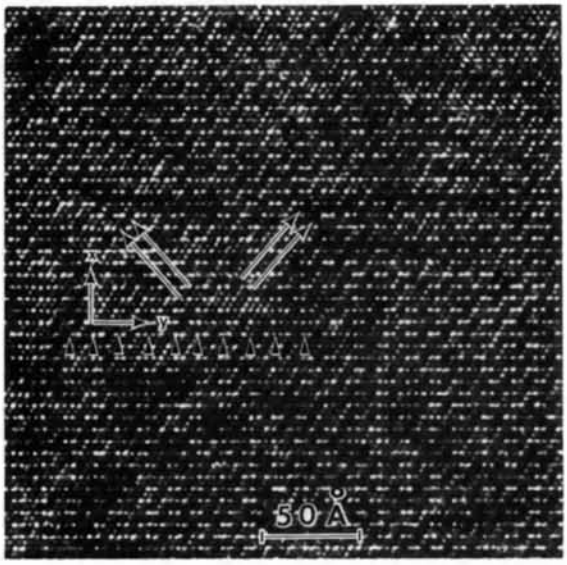

Fig. 5. Image corresponding to the diffraction pattern in Fig. 4(*a*). Arrowheads indicate periodicity corresponding to the spacing of e_1–e_1 reflections; arrows are parallel to the directions of more obvious (one-dimensional) modulation maxima and minima. (View at grazing incidence.)

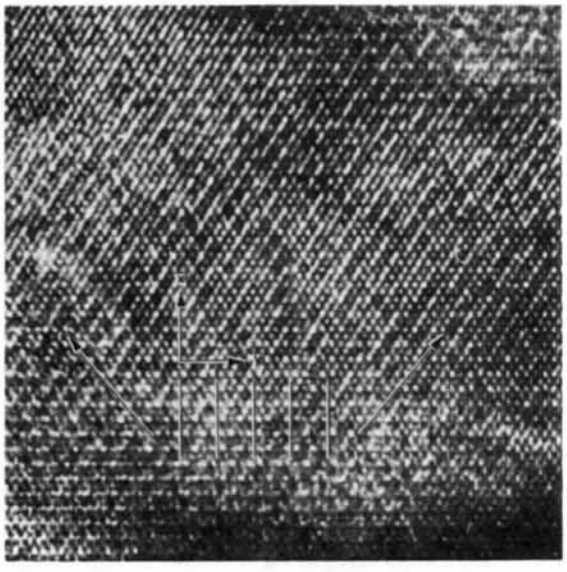

Fig. 6. Another image similar to that in Fig. 5.

Similarly, Fig. 6 is the image corresponding to another $[001]_m$ zone-axis diffraction pattern. The bars indicate and are parallel to the $(010)_m$ modulations. From the image $\Delta = 8{\cdot}1_7$; from the diffraction pattern $\Delta = 8{\cdot}1_4$. The calculated modulation period is therefore $31{\cdot}_3$ and $31{\cdot}_1$ Å respectively. Once again there are two sets of brighter and darker fringes corresponding to reciprocal-lattice vectors between 000 and the two e_1 satellites. In this case they are at $\pm 50°$ to $(010)_m$. Their periodicity (two fringes) on the image is measured as $7{\cdot}_{93}$ Å [$\sim(830)_m$] and $7{\cdot}_{85}$ Å [$\sim(8\bar{3}0)_m$]. (Since all such fringes are close to $\{830\}_m$ and $d\{830\} = 0{\cdot}99$ Å their periodicity $\simeq \Delta$ Å.)

Discussion

The appearance of the satellite reflections is reminiscent of the diffraction patterns of many systems, especially the *e*-plagioclases (Ribbe, 1975; Smith, 1975; McLaren, 1978; McConnell, 1978; Horst, Tagai & Korekawa, 1981; Kumao, Hashimoto, Nissen & Endoh, 1981) from discussions of which the *e*- and *f*-satellite terminology is acquired; but also the pyrrhotites, $Fe_{1-\delta}S$ (*e.g.* Yamamoto & Nakazawa, 1982), CuAuII (Yamamoto, 1982*c*), mullite (Nakajima & Ribbe, 1981), yoderite (Higgins, Ribbe & Nakajima, 1982), *etc.* As already stated, we are dealing with a *modulated crystal structure* (Cowley, Cohen, Solomon & Wuensch, 1979; de Wolff, 1974, 1977, 1981; Böhm, 1975, 1976; Janner & Janssen, 1977, 1979, 1980; Janssen, 1979; Yamamoto, 1982*a*,*b*).

The present example is a relatively simple one: the modulation is one-dimensional. The exact nature of the modulation (occupation density and/or atom displacements) remains to be determined. Its description must be based on the earlier one of Flahaut and co-workers (Domange *et al.*, 1958; Flahaut *et al.*, 1960, 1961) who interpreted their X-ray data from a single crystal of stoichiometry $YbS_{1{\cdot}379} = Yb_{2{\cdot}90}S_4$ (Chevalier, Laruelle & Flahaut, 1967) as indicating a 90% occupancy of the Yb(1) site in the S_6 trigonal prisms, with a random distribution of occupied and unoccupied prisms. (That satellites were not detected in this earlier work is presumably a consequence of their relatively low intensity.) At this stage therefore the most plausible

description is that the basic Yb_3S_4 structure be modified only by modulating the occupancy factor of the trigonal prisms. (It is also likely that some atom displacements will accompany this variation in occupancy and, consequently, cation valence.) The periodicity of the modulation function is approximately $8 \times \mathbf{b}$, usually incommensurate with b, but occasionally commensurate when the 'satellites' become much stronger and greater in number, reminiscent of a normal ('rectangular-wave') superlattice. Its direction is close to {830}; exactly {830} for $\Delta = 8$.

Clearly, a reliable description of the modulation requires single-crystal X-ray analysis of a more carefully prepared sample, probably utilizing the multi-dimensional space-group methods of, *e.g.*, Yamamoto (1982) and de Wolf (1981) for incommensurate structures. (The excessive complexity of our X-ray powder patterns, and the variation of composition with preparation temperature and time all suggest that equilibrium was not achieved.) Attempts to grow single crystals by vapour-phase transport were unsuccessful: I_2, not surprisingly, oxidized Yb^{2+} to Yb^{3+} so that the product was Yb_2S_3; NH_4Cl did not work either.

Because the modulated-structure description still gives an average structure (albeit at a higher level than the original one of random occupancy) high-resolution structure images from the electron microscope are not likely to give as convincing an interpretation of structural details as in the case of well ordered superstructures. This is confirmed by the extensive work on and discussion of the *e*-plagioclases (Morimoto, Kitamura & Nakajima, 1975; Morimoto, Nakajima & Kitamura, 1975; also Kumao, Hashimoto, Nissen & Endoh, 1981). It is likely to be particularly difficult in the present instance because there is no useful, *short* projection axis: the orthorhombic 'unit cell' is $\sim 12{\cdot}7 \times (\Delta \times 3{\cdot}8) \times 12{\cdot}9$ Å $\simeq 13 \times 30 \times 13$ Å.

'High-temperature' preparations

Only a preliminary examination of these has been made. At least three phases are present in one sample; two have been identified. The first is 'Yb_3S_4', electron diffraction patterns of which show only the 'main' reflections characteristic of the $\mathbf{Yb_3S_4}$ structure: there are no satellite reflections. The second has complex diffraction patterns, again clearly consisting of 'main' (strong) reflections and (weaker) satellite or superlattice reflections. But now the latter correspond to a *two*-dimensional modulation. A typical example is given in Fig. 7. The main reflections suggest a superficial resemblance to a $[001]_m$ zone-axis pattern of $\mathbf{Yb_3S_4}$, but it is different: alternate reflections along '$\mathbf{a}_m^*$' are absent (suggesting a halving of 'a') and the axial ratio 'a^*/b^*' is slightly different. One row of the weaker reflections (indicated on Fig. 7) does appear accurately to connect two of the main reflections, and to be commensurate with their spacing. [The reflection is equivalent to $(910)_m$ and the multiplicity is $13\times$, equivalent to $d = 16{\cdot}0$ Å.] The situation is not as simple in any other direction.

It should be emphasized that this type of diffraction pattern is also inconsistent with the $\mathbf{CaTi_2O_4}$-type structure, which has been reported as a high-temperature polymorph of compounds such as CaM_2S_4

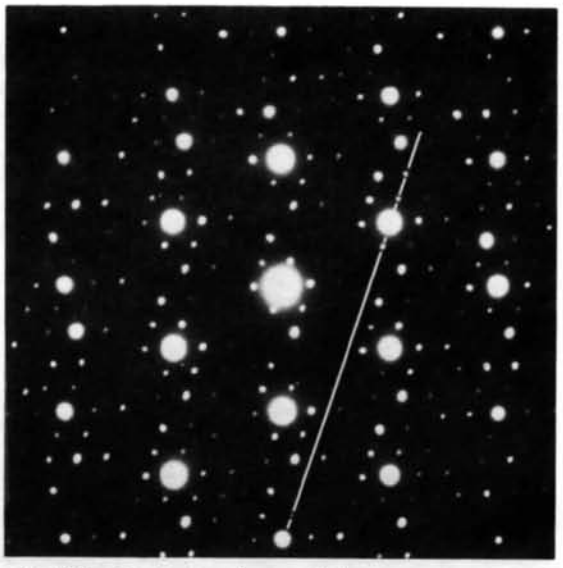

Fig. 7. Diffraction pattern from a high-temperature preparation, with subcell spots superficially resembling those in Fig. 4. But one half of those are absent, and the weaker spots suggest a two-dimensional modulation. The white line indicates a row of spots intersecting the interval between two main spots at intervals of 1/13.

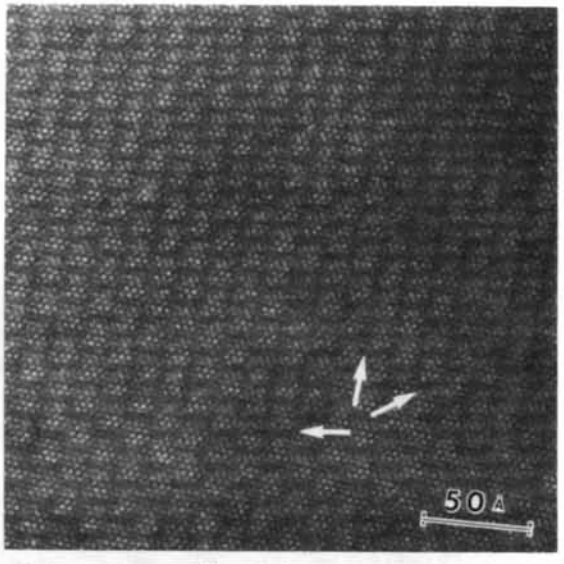

Fig. 8. Image corresponding to Fig. 7. Arrows indicate modulation fringes corresponding to the satellite spots in that figure.

(M = Y, Dy, Ho, Tm, Yb, Lu) which also have the Yb_3S_4-type structure at low temperatures (Patrie & Flahaut, 1967).

Fig. 8 is an image corresponding to the diffraction pattern in Fig. 7. It shows the two-dimensional modulation, with the most obvious modulation fringes in the directions indicated by arrows.

We are grateful to Mr P. Barlow, Dr J. Fitzgerald and Mr N. Ware for assistance with electron microscopy and electron microprobe analysis and to the Spanish Ministry of Science and Education for a supporting grant (to COD).

References

ANDERSSON, S. & HYDE, B. G. (1982). *Z. Kristallogr.* **158**, 119–131.

BAKKER, M. & PLUG, C. M. (1981). *J. Solid State Chem.* **37**, 49–57.

BÖHM, H. (1975). *Acta Cryst.* A**31**, 622–628.

BÖHM, H. (1976). *Z. Kristallogr.* **143**, 56–66.

BOWN, M. G. & GAY, P. (1958). *Z. Kristallogr.* **111**, 1–14.

CHEVALIER, R., LARUELLE, P. & FLAHAUT, J. (1967). *Bull. Soc. Fr. Minéral. Cristallogr.* pp. 564–574.

COWLEY, J. M., COHEN, J. B., SOLOMON, M. B. & WUENSCH, B. J. (1979). Editors. *Modulated Structures*, AIP Conf. Proc. No. 53. New York: American Institute of Physics.

DOMANGE, L., FLAHAUT, J., GUITTARD, M. & LORIERS, T. (1958). *C. R. Acad. Sci.* **247**, 1614–1616.

FLAHAUT, T., DOMANGE, L., GUITTARD, M. & LORIERS, T. (1961). *Bull. Soc. Chim. Fr.* pp. 102–105.

FLAHAUT, T., DOMANGE, L., PATRIE, M. & GUITTARD, M. (1960). *C. R. Acad. Sci.* **251**, 1517–1519.

HIGGINS, T. B., RIBBE, P. H. & NAKAJIMA, Y. (1982). *Am. Mineral.* **67**, 76–84.

HORST, W., TAGAI, T. & KOREKAWA, M. (1981). *Z. Kristallogr.* **157**, 233–250.

HYDE, B. G., ANDERSSON, S., BAKKER, M., PLUG, C. M. & O'KEEFFE, M. (1980). *Prog. Solid State Chem.* **12**, 273–327.

JANNER, A. & JANSSEN, T. (1977). *Phys. Rev. B*, **15**(2), 643–658.

JANNER, A. & JANSSEN, T. (1979). *Physica Sect. A*, **99**, 47–76.

JANNER, A. & JANSSEN, T. (1980). *Acta Cryst.* A**36**, 408–415.

JANSSEN, T. (1979). *J. Phys. C*, **12**, 5381–5392.

KUMAO, A., HASHIMOTO, H., NISSEN, H.-U. & ENDOH, H. (1981). *Acta Cryst.* A**37**, 229–238.

MCCONNELL, J. D. C. (1978). *Z. Kristallogr.* **147**, 45–62.

MCLAREN, A. C. (1978). *Chem. Soc. Spec. Period. Rep.* **7**, 1–30.

MAKOVICKY, E. & HYDE, B. G. (1981). *Struct. Bonding (Berlin)*, **46**, 103–170.

MORIMOTO, N., KITAMURA, M. & NAKAJIMA, Y. (1975). *Proc. Jpn Acad.* **51**, 729–732.

MORIMOTO, N., NAKAJIMA, Y. & KITAMURA, M. (1975). *Proc. Jpn Acad.* **51**, 725–728.

NAKAJIMA, Y. & RIBBE, P. H. (1981). *Am. Mineral.* **66**, 142–147.

PANNETIER, G. & DEREIGNE, A. (1963). *Bull Soc. Chim. Fr.* pp. 1850–1854.

PATRIE, M. & FLAHAUT, J. (1967). *C. R. Acad. Sci.* **264**, 395–398.

RIBBE, P. H. (1975). *Feldspar Mineralogy.* Mineral. Soc. Am. Short Course Notes, 2, R1–R52; Sm.

SMITH, J. V. (1975). *Feldspar Mineralogy.* Mineral. Soc. Am. Short Course Notes, 2, S1–S29.

WOLFF, P. M. DE (1974). *Acta Cryst.* A**30**, 777–785.

WOLFF, P. M. DE (1977). *Acta Cryst.* A**33**, 493–497.

WOLFF, P. M. DE (1981). *Acta Cryst.* A**37**, 625–636.

YAMAMOTO, A. (1982*a*). *Acta Cryst.* B**38**, 1446–1451.

YAMAMOTO, A. (1982*b*). *Acta Cryst.* B**38**, 1451–1456.

YAMAMOTO, A. (1982*c*). *Acta Cryst.* A**38**, 87–92.

YAMAMOTO, A. & NAKAZAWA, H. (1982). *Acta Cryst.* A**38**, 79–86.

Acta Cryst. (1983). B**39**, 575–579

Structure of U–W Oxides Investigated by Means of 1 MV High-Resolution Electron Microscopy

BY N. D. ZAKHAROV, M. A. GRIBELUK AND B. K. VAINSHTEIN

Institute of Crystallography, Academy of Sciences of the USSR, Leninsky Prospekt 59, Moscow 117333, USSR

O. N. ROZANOVA

Moscow State University, Moscow, USSR

AND K. UCHIDA AND S. HORIUCHI

National Institute for Researches in Inorganic Materials, Niihari-gun, Ibaraki, Japan

(*Received* 4 *January* 1983; *accepted* 23 *May* 1983)

Abstract

The structure of U–W oxides with the general chemical formula UW_nO_{3n+2} has been examined by 1 MV high-resolution electron microscopy. The structure models of UW_5O_{17} and UW_4O_{14} are derived from electron microscopy images taken at the 2 Å resolution level. The structures can be regarded as slightly distorted WO_3 slabs sharing U atoms. Intergrowth of WO_3 slabs of different width has been observed. The variation in slab width gave rise to strain fields. Radiation damage due to the action of 1 MV electrons and ions has been observed.

0108-7681/83/050575-05$01.50